Multi-spot focusing by using composite spiral zone plates

Yilei Hua (华一磊)*, Ziqiang Wang (王子强), Hailiang Li (李海亮), Nan Gao (高 南), and Yuchan Du (杜宇禅)

Key Laboratory of Nano-Fabrication and Novel Devices Integrated Technology, Institute of Microelectronics, Chinese Academy of Sciences, Beijing 100029, China

**Corresponding author: huayilei@ime.ac.cn*

Received May 17, 2012; accepted August 7, 2012; posted online November 30, 2012

We present a flexible, simple, and cost effective approach for generating high-quality multiple focal spots in the far field using composite spiral zone plates (SZPs), which serve as a synthesis of two SZPs with different topological charges. By changing the topological charges of the SZPs can obtain different types of multiple focal spots. The numerical solution, fabrication method, and experimental results are presented to prove the capabilities of this approach.

OCIS codes: 050.1965, 230.3990, 050.1380.
doi: 10.3788/COL201210.120502.

Optical vortices, i.e., light beams carrying phase singularities, have attracted significant interest for their unique properties and wide range of potential wide applications[1−3]. In particular, the superposition of two vortex beams with different topological charges generates interesting light structures. These structures are known by various names, such as Ferris wheels[4] and linear azimuthons[5]. Among these light structures, the optical ring lattice is of particular interest[6]. The focal spot of the optical ring lattice presents interesting phenomena, such as multiple focal spots. This unique focal spot has apparent applications in multifocus imaging[7], multiple optical tweezers[8−10], rotating images[11−13], and micro fabrication[14].

Driven by the application demands of multi-spot focusing, various techniques have been proposed and demonstrated for generating multi-spot focus. These techniques include beam splitters to divide the beam into multiple beams[15], phase modulation with a spatial light modulator[16], microlens array[17], and the composite vector beam. Alternatively, diffractive optical elements (DOEs) have emerged as a powerful method for generating optical vortices. DOEs can generate arbitrary complex wavefronts, are low cost, and have simple experimental setup. This letter proposes a single-optical element, termed composite spiral zone plates (CSZPs), to generate high-quality multiple focal spots in the far field. CSZPs serve as a synthesis of two spiral zone plates (SZPs), which are a variation of the Fresnel zone plates (FZPs) with different topological charges[18−20].

To elaborate the design method of CSZPs, we start with investigating the field distribution at the focal plane of a conventional SZP. A SZP is a FZP modified by an addition of linear phase change $l\varphi$ along the angular coordinate, where l is an integer and φ is the azimuthal angle. In accordance with the Huygens's principle, the diffracted electromagnetic (EM) field of a FZP can be derived from the EM field on the FZP's plane. Thus, the diffracted field can be read as

$$\mathrm{d}\mathbf{E}(\mathbf{r}',\mathbf{r}) = [\mathrm{d}\mathbf{s}' \times \mathbf{E}(\mathbf{r}')] \times \frac{\mathbf{r}'-\mathbf{r}}{|\mathbf{r}'-\mathbf{r}|}\frac{\partial}{\partial|\mathbf{r}'-\mathbf{r}|}\Big[\frac{\exp(\mathrm{i}k|\mathbf{r}'-\mathbf{r}|)}{2\pi|\mathbf{r}'-\mathbf{r}|}\Big], \quad (1)$$

where the $\mathrm{d}\mathbf{E}(\mathbf{r}',\mathbf{r})$ is the diffracted field at $\mathbf{r}$ contributed by the source at $\mathbf{r}'$, the differential of the area $\mathrm{d}\mathbf{s}$ is oriented in the direction z, and $\mathbf{E}(\mathbf{r}')$ is the field at $\mathbf{r}'$. The EM field of an l order SZP on the SZPs plane could be written as

$$\mathbf{E}_{\mathrm{szp}} = \mathrm{SZP}_l \times \mathbf{E}_0, \quad (2)$$

where SZP_l stands for the transmission function of the SZPs, and $\mathbf{E}_0$ is the EM field impinging on the SZPs. The transmission function of an l order SZPs is

$$\mathrm{SZP}_l = \frac{1}{2}\Big\{\mathrm{sgn}\Big\{\mathrm{Re}\Big[\exp(\mathrm{i}l\varphi) - 2\mathrm{i}\pi\frac{\sqrt{f^2+\rho^2}-f}{\lambda} + \frac{\mathrm{i}\pi}{2}\Big]\Big\} + 1\Big\}, \quad (3)$$

where f is the focal length of the SZPs, ρ is the radial coordinate in the polar coordinate system, λ is the wavelength, and sgn is the sign function.

With the EM field on the SZP's plane by hand, the field distribution of the focal spot can be calculated directly. Here we calculate an $l = 1$ SZP with 1-cm diameter and the 20-cm focal length, a laser beam with 355-nm wavelength illuminates this SZP. The intensity ($|\mathbf{E}|^2$) and phase of the EM field on the $X-Y$ plane at the focal plane of this SZP are shown in Figs. 1(a) and (b), respectively. The focal spot is evidently ring-shaped, with the minimum at the center. The corresponding phase profile is shown in Fig. 1(b), which is composed of a series of concentric rings. Inside one ring, the phase changes when the azimuth varies, and remains the same when the radius varies. For the $l = 1$ SZP, the amount of the phase change along a circle inside one single ring equals 2π. An abrupt π phase change occurs between the two adjacent rings. Figures 1(a) and (b) show that the focal spot is included in the first ring in Fig. 1(b). Thus, the focal spot of a SZP is a spiral phased ring. This phenomenon gives a clue on how to generate multiple focal spots by the superposition of two spiral-phased rings with opposite topological charges.

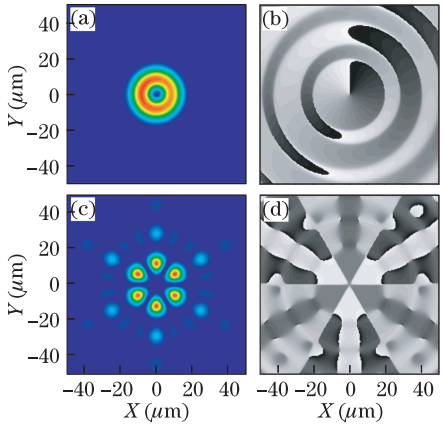

Fig. 1. (a) Intensity and (b) phase distributions of the EM field near the focus of $l = 1$ SZP; (c) intensity and (d) phase distributions of the EM field near the focus of $l = 3$ CSZP.

The EM field of a spiral-phased focus of a SZP could be written in general form as $\mathbf{E}_l(\rho, \varphi) = \mathbf{E}(\rho)\exp(\mathrm{i}l\varphi)$, where ρ is the radius, and $\exp(\mathrm{i}l\varphi)$ stands for the spiral phase. By the superposition of two spiral-phased focal spots with topological charge $+l$ and $-l$, the field distribution of the superposition of the two spiral-phased focal rings can be rewritten as

$$\begin{aligned}\mathbf{E}(\rho, \varphi) &= \mathbf{E}(\rho)[\exp(\mathrm{i}l\varphi) + \exp(-\mathrm{i}l\varphi)] \\ &= \mathbf{E}(\rho)[2\cos(l\varphi)],\end{aligned} \tag{4}$$

and the intensity is

$$I = |\mathbf{E}|^2 = |\mathbf{E}(\rho)|^2 \times 4\cos^2(l\varphi). \tag{5}$$

This intensity distribution represents an angular periodical function with $2l$ knots and can be regarded as $2l$ focal spots.

To generate two spiral-phased focal rings using DOEs, we use an area-divided approach. The whole aperture of this CSZP is divided into multiple sectors. Figures 2(b), (c), and (d) show the images of CSZPs generating 4, 6, and 8 focal spots, respectively. We divide the whole aperture of a SZP into 16, 12, and 16 sectors, accordingly. According to our calculation, removing only one sector of the SZP (this means the sector is opaque) slightly affected the focal spot. The more sectors the SZP is divided into, the less it affects the focal spot. In other words, CSZP exhibits a high degree of fabrication tolerances.

We design an optical element that generates two spiral-phased rings. To do this, we number the sectors of a SZP and remove half of the oddly or evenly numbered sectors (either way does not affect the result). Our numerical calculation shows that the focal spot is almost the same as the original SZP, only with a decrease in intensity. We then fill the removed part of the first SZP with another SZP with an opposite topological charge, resulting in CSZPs, as shown in Fig. 2.

As discussed above, the EM field on the CSZPs plane can be written as

$$\mathbf{E} = \mathbf{E}_0 \times [\mathrm{SZP}_l \times D + \mathrm{SZP}_{-l} \times (1 - D)], \tag{6}$$

where $\mathbf{E}_0$ stands for the EM field impinging on the CSZPs and D represents a sector selection function. Thus, when a sector of SZPs is selected to fit in the CSZPs, $D = 1$. When this sector is not selected, $D = 0$, which can be written in an explicit form:

$$D = \frac{1 + \mathrm{sgn}[\sin(\frac{N\varphi}{2})]}{2}, \tag{7}$$

where φ is the angular coordinate in the polar coordinate system and N is the number of sectors the SZPs are divided into.

Figures 1(c) and (d) show the field intensity and phase distributions of a CSZP to generate 6 focal spots. We are interested in the phase distribution of the multiple focal spots, which is like a cylindrical standing wave. The phase inside each focal spot is a constant, and the phase difference between two adjacent spots is π, indicating that the EM field in two adjacent spots of the first ring vibrates conversely.

To verify further the capabilities of the proposed CSZPs, we fabricate CSZPs by using the conventional microlithography technique. A layer of chromium was deposited on the surface of the glass, spin-coated with photoresist, and exposed by an E-beam writer (Applied Materials Company). The photoresist is developed, and the patterns on the photoresist are transferred to the chromium layer by inductively coupled plasma etching. In our proof-of-principle experiments, the focal length of the CSZPs is 20 cm, and the diameter is 1 cm. The NA of the CSZP is 0.025. The CSZP comprises 176 transparent zones.

The microscopic images of the fabricated CSZPs are shown in Fig. 2. Figure 2(a) is a conventional +2 order SZP that we use for comparison. Figure 2(b) is designed to obtain 4 focal spots and is, thus, divided into 16 sectors. Half of the sectors are filled with SZPs with topological charge +2 and the other half sectors are filled with SZPs with topological charge –2. Figures 2(c) and (d) show the DOEs designed to obtain 6 and 8 focal spots, respectively. The topological charges of the SZPs in Fig. 2(c) are +3 and –3, whereas the charges are +4 and –4 in Fig. 2(d).

The experimental optical system is schematically illustrated in Fig. 3. We use a 355-nm laser (DC50H-35, Spectra-Physics) as the light source. An inverted

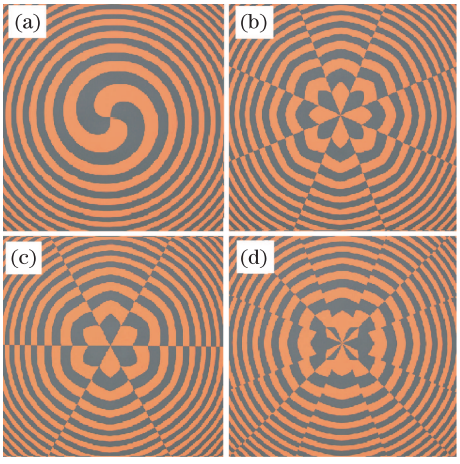

Fig. 2. Microscopic images of (a) a conventional SZPs and CSPZs to generate (b) 4, (c) 6, and (d) 8 focal spots, respectively.

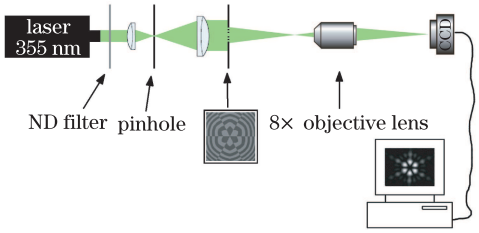

Fig. 3. Experimental setup for optical CSZP demonstration.

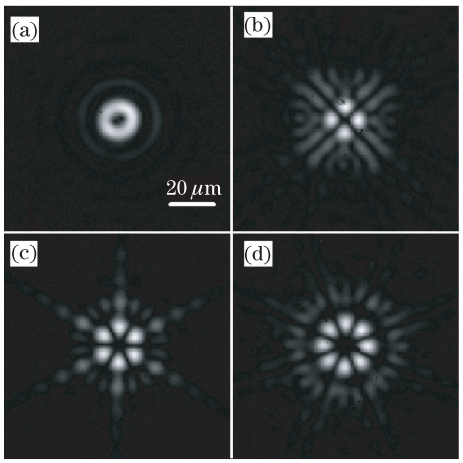

Fig. 4. Focal spots of (a) a conventional l= 2 SZPs and CSZPs designed to generate (b) 4, (c) 6, and (d) 8 spots, respectively.

telescope expands and collimates the laser beam. When necessary, a neutral density (ND) filter is inserted to weaken the power of the light. The pinhole in this telescope is rather small. Thus, the light impinging on the CSZP serves as a plane wave. The focal spot patterns are captured by a charge coupled device (CCD, lumenera LW230) camera through an 8× objective lens.

The experimentally measured images are shown in Fig. 4. Four, six, and eight focal spots are shown in Figs. 4(b), (c), and (d), respectively. The field patterns shown in Fig. 4(c) coincide well with the numerical results shown in Fig. 1(c), proving the validity of the proposed CSZPs in realizing multi-spot focusing and the feasibility of our fabrication process. According to our calculation, the diffraction efficiency of three CSZPs for 4, 6, and 8 foci are 2.5%, 2.0%, and 1.8%, respectively. The intensity variation of the foci for these CSZPs is less than 1%.

In conclusion, we propose a method that is capable of generating multiple focal spots using a single-optical element. The CSZPs are designed for the superposition of two spiral-phased rings for the generation of multiple focal spots. Both numerical and experimental results demonstrate the effectiveness of this approach. The proposed CSZPs have various potential applications in micromanipulation, multifocus imaging, lithography, etc.

References

1. S. N. Khonina, V. V. Kotlyar, R. V. Skidanov, V. A.Soifer, K. Jefimovs, J. Simonen, and J. Turunen, J. Mod. Opt. **51,** 2167 (2004).
2. C. Xie, X. Zhu, and J. Jia, Opt. Lett. **34,** 3038 (2009).
3. C. Xie, X. Zhu, L. Shi, and M. Liu, Opt. Lett. **35,** 1765 (2010).
4. S. Franke-Arnold, J. Leach, M. Padgett, V. Lembessis, D. Ellinas, A. Wright, J. Girkin, P. Ohberg, and A. Arnold, Opt. Express **15,** 8619 (2007).
5. A. Bekshaev and M. Soskin, Opt. Lett. **31,** 2199 (2006).
6. P. Vaity and R. P. Singh, Opt. Lett. **36,** 2994 (2011).
7. L. Sacconi, E. Froner, R. Antolini, M. R. Taghizadeh, A. Choudhury, and F. S. Pavone, Opt. Lett. **28,** 1918 (2003).
8. W. M. Lee, X.-C. Yuan, and D. Y. Tang, Opt. Express **11,** 199 (2003).
9. L. Paterson, M. P. MacDonald, J. Arlt, W. Sibbett, P. E. Bryant, and K. Dholakia, Science **292,** 912 (2001).
10. B. P. S. Ahluwalia, X.-C. Yuan, K. J. Moh, and J. Bu, Appl. Phys. Lett. **91,** 171102 (2004).
11. V. V. Kotlyar, V. A. Soifer, and S. N. Khonina, J. Mod. Opt. **44,** 1409 (1997).
12. P. Pääkkönen, J. Lautanen, M. Honkanen, M. Kuittinen, J. Turunen, S. N. Khonina, V. V. Kotlyar, V. A. Soifer, and A. T. Friberg, J. Mod. Opt. **45,** 2355 (1998).
13. V. V. Kotlyar, S. N. Khonina, R. V. Skidanov, and V. A. Soifer, Opt. Commun. **274,** 8 (2007).
14. X. Sun, C. Zhou, H. Ru, Y. Zhang, and B. Yu, Chin. Opt. Lett. **2,** 4 (2004).
15. A. Cheng, J. T. Gonçalves, P. Golshani, K. Arisaka, and C. Portera-Cailliau, Nat. Meth. **8,** 139 (2011).
16. K. Obata, J. Koch, U. Hinze, and B. N. Chichkov, Opt. Express **18,** 17193 (2010).
17. J. Bewersdorf, R. Pick, and S. W. Hell, Opt. Lett. **23,** 655 (1998).
18. N. R. Heckenberg, R. McDuff, C. P. Smith, and A. G. White, Opt. Lett. **17,** 221 (1992).
19. D. Cojoc, B. Kaulich, A. Carpentiero, S. Cabrini, L. Businaro, and E. Di Fabrizio, Microelectron. Eng. **83,** 1360 (2006).
20. A. Sakdinawat and Y. Liu, Opt. Lett. **32,** 2635 (2007).